Title
THE EROSIVTTY OF COAL PARTICLES IN COAL-SOLVENT SLURRIES

Authors
Levy, A.
Jee, N.
Sorell, G.

Publication Date
1984-06-01

Lawrence Berkeley Laboratory
UNIVERSITY OF CALIFORNIA

Materials & Molecular
Research Division

Presented at the ASTM International Symposium of Slurry Erosion: Uses, Applications and Test Methods, Denver, CO, June 26-27, 1984

THE EROSIVITY OF COAL PARTICLES IN COAL-SOLVENT SLURRIES

A. Levy, N. Jee, and G. Sorell

June 1984

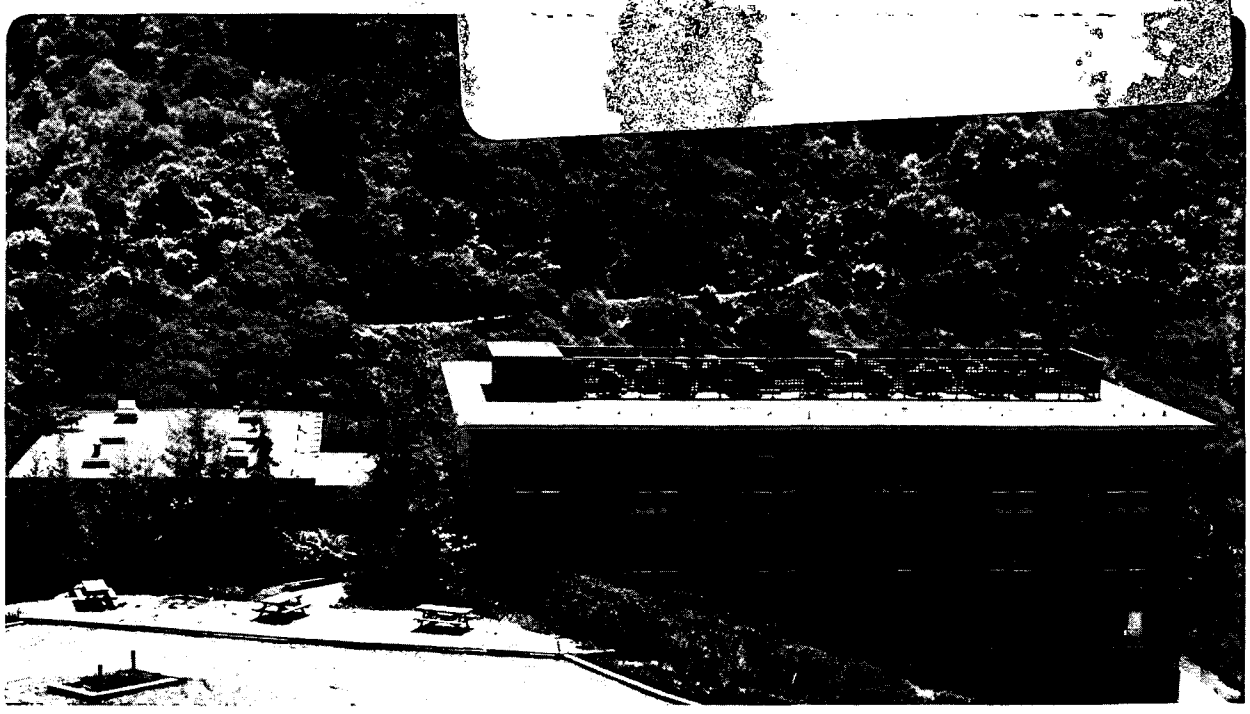

Prepared for the U.S. Department of Energy under Contract DE-AC03-76SF00098

DISCLAIMER

LBL 17908

THE EROSIVITY OF COAL PARTICLES IN COAL-SOLVENT SLURRIES

by

A. Levy and N. Jee

Lawrence Berkeley Laboratory
University of California
Berkeley, California 94720

G. Sorell

Exxon Research & Engineering Company
Florham Park, New Jersey 07932

Research sponsored by the US Department of Energy under DOE/FEAA 15 10 10 0, Advanced Research and Technical Development, Fossil Energy Materials Program, Work Breakdown Structure Element LBL- 3.5 and under Contract No. DE-AC03-76SF00098.

ABSTRACT: An investigation of the erosivity of particles of several different coals and respective vacuum bottoms from the Exxon Donor Solvent (EDS) coal liquefaction pilot plant Exxon Coal Liquefaction Process (ECLP) was carried out. Kerosene and tetrahydrofuran (THF) were used as the liquids in slurries containing 30 wt% particles. The particles were of several sizes, shapes, integrities (fracture strengths) and ash contents. It was determined that the primary factors having a direct effect on erosivity were particle size, and ash content/composition. Particle shape and resistance to fracturing upon impact had important secondary effects. All of these factors are interrelated and can counter each other under certain conditions. Slurry pot testing proved valuable as a reproduceable method for comparative erosion studies, but should not be relied upon to produce quantitative erosion data for equipment design purposes.

Introduction

Many different coals will be used in coal liquefaction plants, each containing different compositions and quantities of erosive mineral matter. It is the ash or mineral matter in coal that is primarily responsible for the erosion of the metal containment surfaces of the equipment through which the coal slurries flow. [1,2] The carbonaceous matter in coal has very little erosivity. The composition, quantity, morphology, size, shape and location of the ash particles in the coals and the same properties of ash particles that have been released from the coal are the variables that determine the erosivity of coal-solvent slurries. The purpose of this investigation

was to determine the erosivity of hydrocarbon based slurries containing ground coal or ash-rich vacuum bottoms obtained from ECLP, the 250 ton/day EDS coal liquefaction pilot plant in Baytown, Texas.

The erosivity of several oxides, some of which are contained in coal, has been studied in gas-solid particle erosion. [3] It was determined in these tests that the weaker oxides, as assessed by their hardness, fractured upon impact and, as a result, were much less erosive than the stronger oxides which did not. It was also determined that the shape of the erosive particles had a significant effect on their erosivity, with angular particles being considerably more erosive than spherical particles. The size, shape and location of the oxides in the ground coal particles were related to the effect that they had on the metal being eroded in Reference 4. Figure 1 [4] shows that the carbonaceous constituents of the coal (dark) hold the mineral constituents (white) much as a tool holder maintains the position of a tool. The resultant imprint of the oxide particles in the target metal surface have the same shape as the mineral constituents in the coal. It is by this means that the finely divided, hard oxides in the relatively soft coal cause the coal particles to be erosive.

The size of the coal particles is another factor that has been shown to be directly related to their erosivity. [5] The mass of each coal particle directly relates to its kinetic energy as it impacts an eroding surface. The larger coal particles, therefore, have a greater capacity to drive the mineral particles in their surfaces into the target. Thus, even with very fine sized mineral particles embedded in much larger size coal particle "tool holders", the erosivity of a

slurry can be related to the overall size of the coal particles.

Another size factor that affects the overall erosivity of a coal mixture is the presence of oxide contaminant particles such as SiO_2 that are separate from the coal but that have the same size as the coal particles. Coal cleaning operations remove a high percentage of these particles, but not all of them. The remaining mineral particles have a considerably greater erosivity than the ash containing coal particles of the same size and probably account for the principal amount of erosion that occurs. Figure 2 shows a typical eroded surface of 304SS when -200 mesh size coal was used in a kerosene-coal slurry. [6] The large crater that can be seen on the right side of the photo was caused by a single oxide particle probably SiO_2 or Al_2O_3, the size of the coal particles. The much greater erosive effect of the larger size mineral particle compared to the "paw prints" of ash contained in the coal particles can be seen. Figure 2 is of an area near the periphery of the eroded zone when a jet impingement tester was used.

Another possible aspect of the effect of particle size is the ability of the large size particles to offset the particle defeating function that the viscosity and lubricity of the carrier liquid plays in slurry erosion. Their greater mass will result in their ability to drive through the carrier liquid to the eroding surface more effectively.

With this understanding of the nature of coal-solvent slurry erosion, the different ECLP coals and vacuum bottoms that were to be utilized in the laboratory slurry pot tests were selected to provide a range of different sizes and mineral contents. Their erosivity was

studied in coal-kerosene and vacuum bottoms-tetrahydrofuran (THF) slurries. THF was chosen because it is a highly effective solvent for carbonaceous coal residues. THF has about the same viscosity as kerosene.

Test Conditions

The coal and ground agglomerated vacuum bottoms were shipped from ECLP in metal cans without de-humidifiers. The compositions of the coals and derived vacuum bottoms are listed in Tables 1 and 2 respectively. The particles that did not readily pour from the cans or that showed evidence of clumping due to their moisture content were dried prior to being mixed into a slurry by passing air over shallow trays of the particles for 2 hours at 105°C. Particle size distributions listed in Tables 4 and 5 were determined by sieve analyses using a Rotap Machine and a set of Tyler Sieves. Efforts to determine particle size distribution using a laser detector were not successful because the particles tended to float on top of the liquid carrier used in the laser apparatus.

The coal particles and the vacuum bottoms were prepared into 30 wt% particle-kerosene slurries by mixing the two constituents in the slurry pot prior to testing. Additionally, some erosion experiments with vacuum bottoms were conducted with slurries synthesized with THF instead of kerosene. The rationale for using this more effective solvent was to dissolve the ash agglomerates to attain smaller particle sizes, approaching the microscopic ash-rich particles existing in hot, liquid vacuum bottoms streams during plant operation.

The erosion tests were carried out in a slurry pot tester which is described in Reference 3. It consists of a baffled, stirred 3 liter cylindrical container. Attached to the 3/4 HP motor driven central shaft are two specimen holding arms rotating the specimens in a 105 mm diameter circular path at effective velocities from 6-15 m/s. The specimens were cold rolled 1018 steel rods 0.3 cm. dia. by 5 cm. long and 1018 steel rods of the same size annealed at 850°C for 45 minutes and slow cooled. The effective velocity of the slurry was 12 m/s. Test temperature was maintained at 28°C and the test duration was held to two hours. The decision to limit conditions to a single velocity, temperature and test material was based on earlier work with the slurry pot which showed that changing these parameters affected erosion to a predictable or minor extent. [5]

Results and Discussion

Particle Analysis

Analyses of the ECLP coals and vacuum bottoms listed in Tables 1 and 2 were determined by Exxon Research and Engineering Company. The batch of Lawrence Berkeley Laboratory (LBL) Illinois No. 6 coal, also used in this study, was obtained at an earlier time from another source. The chemical composition of the LBL sample was not determined; however, it can be reasonably assumed that the analysis of the ECLP coal is generally representative for the LBL Illinois No. 6 coal as well.

All the coals have fairly similar carbonaceous content but differ appreciably in ash (mineral) content. As shown in Table 3, there are also pronounced differences in the relative amounts of constituent oxides in the ash. The high ash Martin Lake Lignite contains by far the greatest proportion of mineral matter. Vacuum bottoms are about twice as rich in ash as the raw feed coal being liquefied. However, the minerals composition in the bottoms ash stays essentially the same as in the coal since the process conditions in hydroliquefaction are too mild to decompose stable oxides.

Differences in ash content can be directly related to the erosion data obtained in the slurry pot tests. The much weaker carbonaceous materials in the coals account for little of their erosivity, directly, even though they account for $\sim$ 90 wt% of the coal. The principal function of the carbonaceous material in the coal particles is to provide the mass necessary to drive the mineral constituents in them into the surface being eroded.

It is shown in Table 1 that the highest ash content coal was the Martin Lake Texas lignite. The other three coals tested had approximately half that amount of ash in them. Also important to the erosivity of the coal are the amounts of the various oxides that constitute the ash. The stronger oxides, as represented by their listed hardnesses in Table 3 do not fracture into small pieces when they impact the surface, and therefore can affect a larger area on the eroding surface as the result of their larger size. [3] Thus, the greater the content of such oxides as SiO_2 and Al_2O_3 in the coal, the more erosive it is likely to be. It can be seen that the high ash

content lignite has the largest amount of combined silica and alumina (73%). The Illinois No. 6 coal has the second highest content of these two minerals (70.4%) while the other coals have considerably lower amounts.

The shape and distribution of the oxides in the coal also have a strong influence on the erosivity of the coal particles. Petrographic analysis of the coals as shown in Figure 1 is used to determine this distribution. Unfortunately, this type of analysis was not available for the specific coals tested in this project. Therefore, the nature and effectiveness as erodents of the ash distribution in the coals tested had to be assessed by the resultant erosion rates of the 1018 steel.

The particle size distribution of the coals and vacuum bottoms is shown in Tables 4 and 5. There is a significant amount of small particles, <50μm, in three of the coals tested. The small particles in these fine grinds probably have a minimum effect on the erosivity of the coals. It is the relatively small percentage of coarser particles, >100μm, that presumably cause the major amount of the erosion. As will be shown later, it was the coarse coal and vacuum bottoms slurries that proved to be the most erosive.

Coal Erosion

The erosion rates of the 1018 steel were plotted in two ways, showing either cumulative or incremental metal loss. Curves showing cumulative erosion were prepared by measuring the total amount of weight loss that had occurred over the front half surface area of the

rod specimens up to the selected test time and plotting it against the test time. Figure 3 shows this type of a curve for two specimens tested simultaneously in the slurry pot. In incremental erosion rate plots, the weight loss incurred for each increment of test time is plotted. Thus each data point represents the amount of loss that had occurred since the last weighing time divided by the elapsed time to obtain the rate of erosion. Figure 4 shows an incremental erosion rate plot for the same two specimens plotted in Figure 3.

In Figure 3, the erosion caused by the large particle size Illinois No. 6 is plotted. A relatively large amount of weight loss occurred after two hours of exposure. The small curvature in the plot for the first 45 minutes of testing is attributed to some comminution of the particles as they struck the metal surface, breaking off some angular protrusions and generally, decreasing in size by 25-50%. The surface texture of the coal particles before and after testing was the same indicating no polishing of the particles.

The incremental erosion rate curve shown in Figure 4 provides greater insight into the erosion process that is occurring than the cumulative plot in Figure 3. The high rate of erosion early in the test is the result of three complimentary effects. They are: (1) the progressive cold working of the surface as the result of the plastic deformation of the steel by the impacting particles [7] (2) the comminution of the coal particles and (3) the polishing effect that occurs early in the test when the higher, more vulnerable protrusions of metal are knocked off the surface. As the surface work hardens, the erosion rate decreases. After about 2 hours of exposure, the eroding

surface is reaching a steady state condition where the cold work surface reaches its maximum hardness, the erodent particles reach a constant size and shape, and the initial metal protrusions have been removed. Subsequent increments of particle impacts of the same quantity will cause equivalent amounts of erosion to occur.

Smaller erodent particles cause considerably less erosion to occur. Figure 5 shows the erosion curves from the LBL Illinois No. 6 coal and the ECLP Wyoming coal tests, both of which had the same average particle size, 65μm. The Illinois No. 6 coal was more erosive than the Wyoming coal but caused only 1/10 the erosion that resulted from the same Illinois No. 6 coal that had a 443μm average particle size.

The incremental erosion rate curves for the two small size coals are shown in Figure 6. The typical shape of the curve shown in Figure 4 also occurs when smaller size erodent is used. The small weight loss experienced by the 1018 steel when it was eroded by the Wyoming coal made it difficult to obtain consistent weight loss measurements, thereby accounting for the greater spread in the data points for this coal in Figure 6. It appears that the lower erosivity Wyoming coal causes the 1018 steel to reach steady state conditions sooner than does the more erosive Illinois No. 6 coal. The Wyoming coal causes considerably less erosion than the Illinois No. 6 coal early in the test. Their rates will become closer together after the Illinois No. 6 coal causes the 1018 to reach steady state conditions, primarily because of the same particle size of both coals.

The slope of the incremental erosion rate curve for the 65μm size

Illinois No. 6 coal from 30 min. to 120 min. shown in Figure 6 is considerably less than that of the curve for the 443μm size Illinois No. 6 coal plotted in Figure 4. This difference is due to the considerably less comminution that occurred for the smaller size particles and the decreased amount of work hardening of the steel surface that the lower mass, smaller particles caused.

The marked effect on erosion of the ash content of the coal is illustrated in Figure 5 showing erosion losses for three different coals having comparable particle sizes. The direct relationship between ash composition and erosion is shown in Figure 7 which is a cross plot of the cumulative 120 minute erosion losses of these three coals versus their silica plus alumina ash content. The same effect is observed when the incremental, steady state erosion rates for the three coals are plotted. However the curve is more assymptotic as the SiO_2 and Al_2O_3 content increases. ECLP experience confirms this relationship to the extent that erosion was observed to be considerably more severe during high ash lignite operation than when lower ash coals were run.

Vacuum Bottoms Erosion

The vacuum bottoms of the three test coals from ECLP pilot plant were investigated in both their agglomerated and separated particle conditions. Kerosene was used as the slurry liquid in the agglomerated particle test. The agglomerates, which consisted of ground solidified bottoms, were separated by using THF solvent as the slurry liquid which dissolved the carboneous material. The ash that has been released from the coal in the liquefaction process is concentrated in the vacuum

bottoms, (see Table 2). Thus, the vacuum bottoms can be expected to be more erosive than the coals themselves. However, particle size, integrity and shape also affected the erosivity of these particles.

Figure 8 plots the incremental erosion rates of the 1018 steel by the agglomerated vacuum bottoms from the Illinois No. 6 and Wyoming coals. The large size particles (see Table 5) and their high ash contents (see Table 2) resulted in nearly the same erosion rates throughout the test period. The steady state incremental erosion rates for the small size Illinois No. 6 coal (Figure 6) and its larger size vacuum bottoms (Figure 8) are nearly the same, considerably lower than the steady state rate for the large size Illinois No. 6 coal (Figure 4). This is probably due to comminution of the vacuum bottoms during the two hour test as the particles are really agglomerates of much smaller size particles. As these agglomerates are broken down as the result of their repeated impacts on the 1018 steel in the slurry pot, they become both smaller in size [5] and more round in shape as their sharper corners are broken off. Both changes reduce their erosivity [3,5]. The two changes combine to offset the increased erosivity from the high ash content and higher starting particles size of the vacuum bottoms. The result is the steady state vacuum bottoms erosivity of the Illinois No. 6 and Wyoming coals being about the same as that of the coals themselves. While these compensating factors may explain the comparable erosion rates obtained with coals and vacuum bottoms in slurry pot testing, the behavior may not necessarily hold for real plant conditions.

The difference in the erosivity of the 38 wt% high ash and 22 wt% low ash content Martin Lake Texas lignites vacuum bottoms at their actual particle size, unagglomerated, is best seen in the cumulative erosion curve, (Figure 9). In a THF solvent slurry, the high ash lignite vacuum bottoms have caused considerably more erosion to occur in the 1018 steel than the low ash lignite vacuum bottoms. The amount of erosion caused by the small, individual particles of low ash lignite vacuum bottoms plotted in Figure 9 after two hours of rotation of the specimens in the slurry pot tester is 14 g/cm^2x10^{-4}. The agglomerated form of the same vacuum bottoms tested in kerosene had caused 115 g/cm^2x10^{-4} to occur after two hours of testing. Thus, the effect of particle size can readily be seen.

The comminution of the vacuum bottoms can also be assessed by comparing the amount of erosion after two hours of testing of the large size, agglomerated lignite vacuum bottoms, 115 g/cm^2x10^{-4} to the 140 g/cm^2x10^{-4} amount of erosion which was caused by the Illinois No. 6 coal (Figure 3). The lignite has twice the concentration of ash, 22% compared to 10.9% for the Illinois No. 6 coal, and, therefore, a greater potential erosivity. However, the greater integrity or fracture strength of the Illinois No. 6 coal particles result in their maintaining their size and shape better after two hours of testing than do the weaker, agglomerates of lignite vacuum bottoms, resulting in a greater total amount of erosion of the 1018 steel by the coal. As discussed above, it appears that in the case of these two kinds of particles, the particle size and shape effects have more influence on the erosivity of the slurry than does the ash content of the particles.

While this may hold true for kerosene base slurries, the situation could change with prolonged testing in THF slurries and real plant streams because of more effective exposure of the abrasive ash particles due to "chemical comminution".

Conclusions

1. The erosivity of coals and vacuum bottoms are affected by the particle size, shape, integrity and ash content/composition of the particles.

2. Particle size is a dominant factor in coal slurry erosion. In the range investigated, a 7-fold increase in particle size resulted in a 10-fold increase in erosion.

3. Ash content/composition is another important factor influencing coal slurry erosion. Indications are that erosion is roughly proportional to combined SiO_2 and Al_2O_3 content.

4. Particle shape and integrity or fracture strength also play a role, with angular, strong particles being more erosive than rounded, frangible ones.

5. Vacuum bottoms slurry erosion appears to be governed by the same factors as raw coal slurries. For more realistic simulation of plant slurries, THF solvent is preferable to kerosene although it is more difficult to use in the laboratory.

6. Incremental erosion rate curves are superior to cumulative erosion loss curves for analyzing and interpreting test results.

7. The factors affecting the erosivity of the particles can be traded off with the resulting erosivity being higher or lower, depending upon which of the factors noted above predominate.

8. The slurry pot is a useful device for conducting mechanistic and comparative erosion studies but cannot be relied upon for producing quantitative, design erosion rate data.

Research sponsored by the U.S. Department of Energy under DOE/FEAA 15 10 10 0, Advanced Research and Technical Development, Fossil Energy Materials Program, Work Breakdown Structure Element LBL-3.5 and under Contract No., DE-AC03-76SF00098.

REFERENCES

1. Lendvai-Lintner, E., Jones, J.P., Sorell, G., "Erosion Experience at the EDS Coal Liquefaction Pilot Plant", Proceedings of NACE Conference on Corrosion-Erosion-Wear of Materials in Emerging Fossil Energy Systems, pp. 155-178, Berkeley, CA, January, 1982.

2. Jones, J.P., Buchheim, G.M., Lendvai-Lintner, E., Sorell, G., "Materials Performance in the EDS Coal Liquefaction Pilot Plant", Paper No. 80, NACE, Corrosion/84, New Orleans, LA, April, 1984.

3. Levy, A.V. and Chik, P., "The Effects of Erodent Composition and Shape on the Erosion of Steel", Wear 89 No. 2, pp. 151-162, August, 1983.

4. Sargent, G.A., Spencer, D.K.., Saguez, A.A., "Slurry Erosion of Materials", Proceedings of NACE Conference on Corrosion-Erosion-Wear of Materials in Emerging Fossil Energy Systems, pp. 196-231, Berkeley, CA, January, 1982.

5. Levy, A.V. and Hickey, G., "Surface Degradation of Metals in Simulated Synthetic Fuels Plant Environments", Paper No. 154 NACE, Corrosion/82, Houston, TX, March, 1982.

6. Levy, A. and Yau, P., "Erosion of Steels in Liquid Slurries". Report No. LBL-15658, Lawrence Berkeley Laboratory, University of California, Berkeley, CA 94720. December, 1983 - Submitted to WEAR.

7. Levy, A., Yau, P., and Jee, N., "Erosion of Steels in Coal-Solvent Slurries", Paper No. 83, NACE, Corrosion/84, New Orleans, LA, April 1984.

Table 1 Coal Compositions

Coal Rank	Illinois #6 Bituminous	Wyoming Subbitum-inous	Martin Lake Low Ash Lignite	Martin Lake High Ash Lignite
Ash (dry wt%)	10.9	9.3	9	23
Carbonaceous materials				
Element Analysis (dry wt%)				
Carbon	69.1	68.3	67.4	57.0
Hydrogen	5.0	4.8	4.8	4.1
Oxygen	9.4	16.0	16.6	13.9
Nitrogen	1.3	1.0	1.4	1.1
Sulfur	4.3	0.6	0.8	0.9
Total wt% of coal	100.0%	100.0%	100.0%	100.0%
SO_3 wt% of ash	3.1%	18.0%	14.8%	6.2%

Table 2 Vacuum Bottoms Compositions

	Illinois #6	Wyoming	Martin Lake Low Ash	Martin Lake High Ash
Ash (dry wt%)	20.8	22.3	22.1	38.3
Sulfur (dry wt%)	2.7	0.8	0.9	1.0

Elemental Analyses: Assumed to be in same proportion as for coal.

Table 3 Ash Analysis

Ash Element Analyses SO_3 free dry wt%			Illinois #6	Wyoming	Martin Lake Low Ash	Martin Lake High Ash
	Hardness	Kg				
Oxide	Moh	VH mm				
SiO_2	7	700	51.6	41.2	41.2	59.7
Al_2O_3	9	1900	16.8	18.7	16.8	13.3
Fe_2O_3	6.8	755	19.2	6.3	11.5	6.8
CaO	4.0-4.5	163-370	4.4	23.9	20.8	13.2
MgO	5.0-6.5	430-690	1.1	5.9	6.8	3.3
TiO_2	5-6.5	430-690	0.9	1.2	1.3	1.6
Na_2O	-	-	1.3	1.1	1.2	0.9
K_2O	-	-	2.4	0.6	0.2	0.5
P_2O_5	-	-	0.3	1.1	0.2	0
Total wt% of ash elements			100.0%	100.0%	100.0%	100.0%

Table 4 Coal Particle Size Distribution

Particle Size	ECLP Illinois #6	LBL Illinois #6	ECLP Wyoming	ECLP Martin Lake Low Ash	ECLP Martin Lake High Ash
>701μm	26.7				
701-425μm	23.3				
425-250μm	17.8				
>300μm		0	0	0.16	0.08
300-150μm		0.1	0.08	2.69	0.72
250-180μm	9.2				
<180μm	23.0				
150-90μm		3.2	13.08	13.95	10.06
90-38μm		67.5	61.97	68.27	62.25
<38μm		29.2	24.87	14.93	26.89
	100.0%	100.0%	100.0%	100.0%	100.0%
Average Particle Size	443μm	65μm	65μm	73μm	65μm

Table 5 Vacuum Bottoms Particle Size Distribution (agglomerated condition)

Particle Size	Illinois #6	Wyoming	Martin Lake Lignite Low Ash
>701μm	10.6	15.6	10.2
701-425μm	18.4	23.2	18.3
425-250μm	21.6	22.2	21.4
250-80μm	11.3	10.2	11.2
<180μm	38.11	28.8	38.9
	100.0%	100.0%	100.0%
Average Particle Size	344μm	389μm	341μm

FIGURES

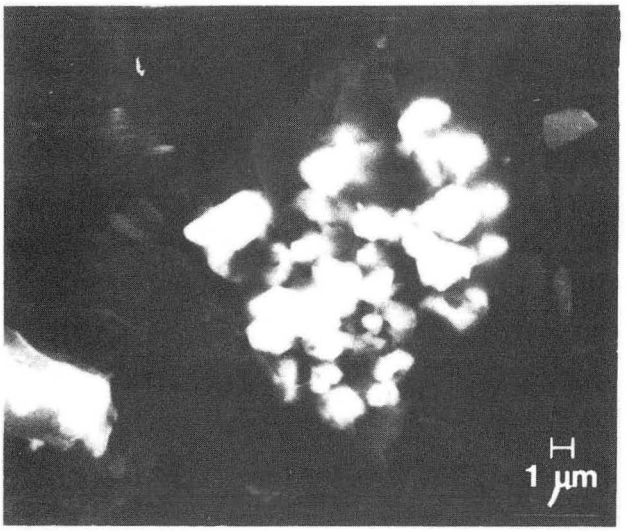

PYRITE ON
COAL SURFACE

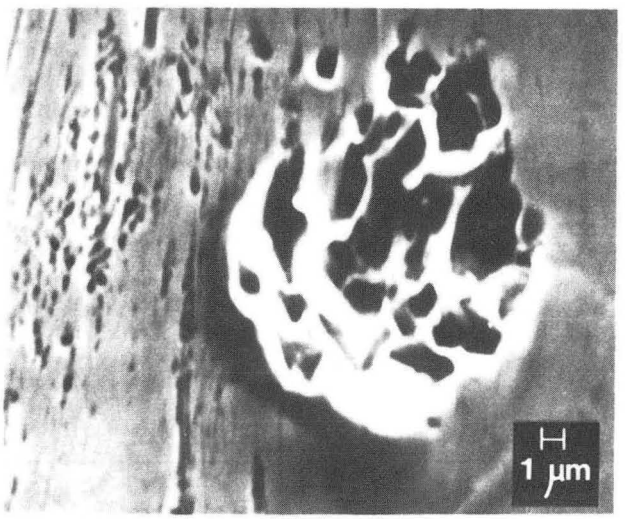

IMPRINT ON
1050 C.S. SURFACE

30° IMPACT
18 m/s

Fig. 1. Pyrite crystallites in coal and impression in eroded steel.

XBB 835-3893

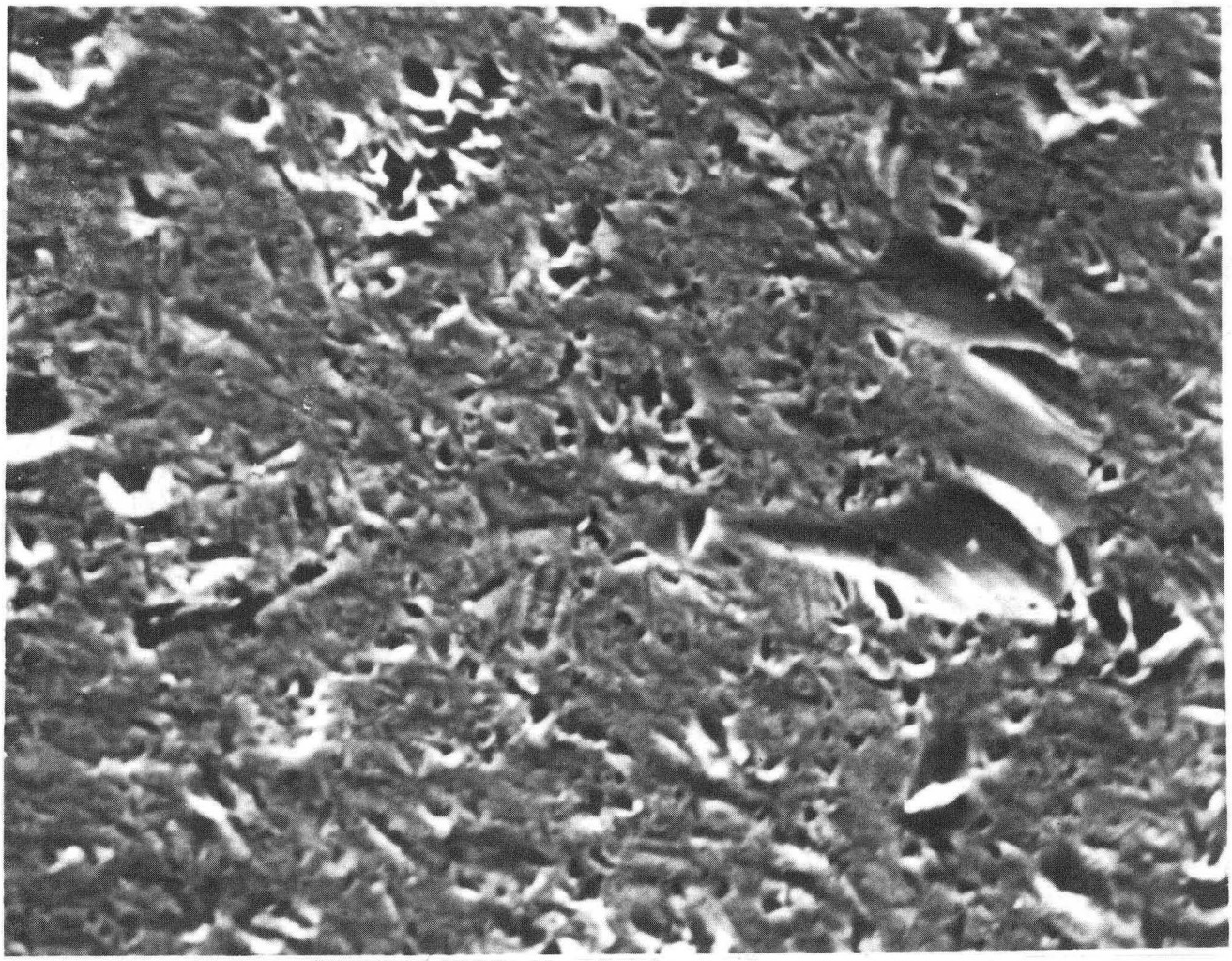

Fig. 2. Eroded surface showing effects of sand particles and coal particles.

XBB 819-9061

5 μm

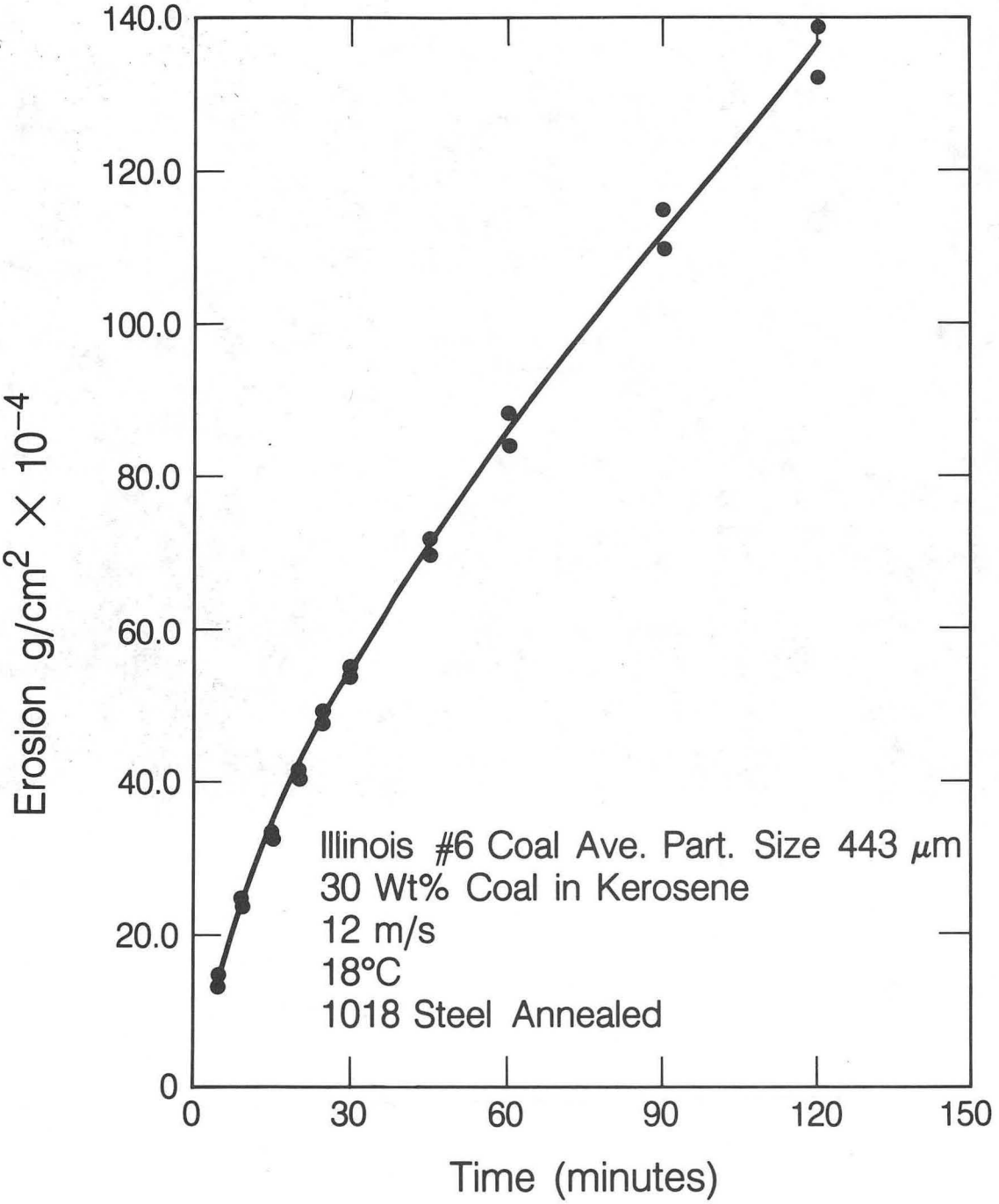

Fig. 3. Cumulative erosion of 1018 steel by 443μm average diameter Illinois No. 6 coal particles in kerosene.

XBL 846-8970

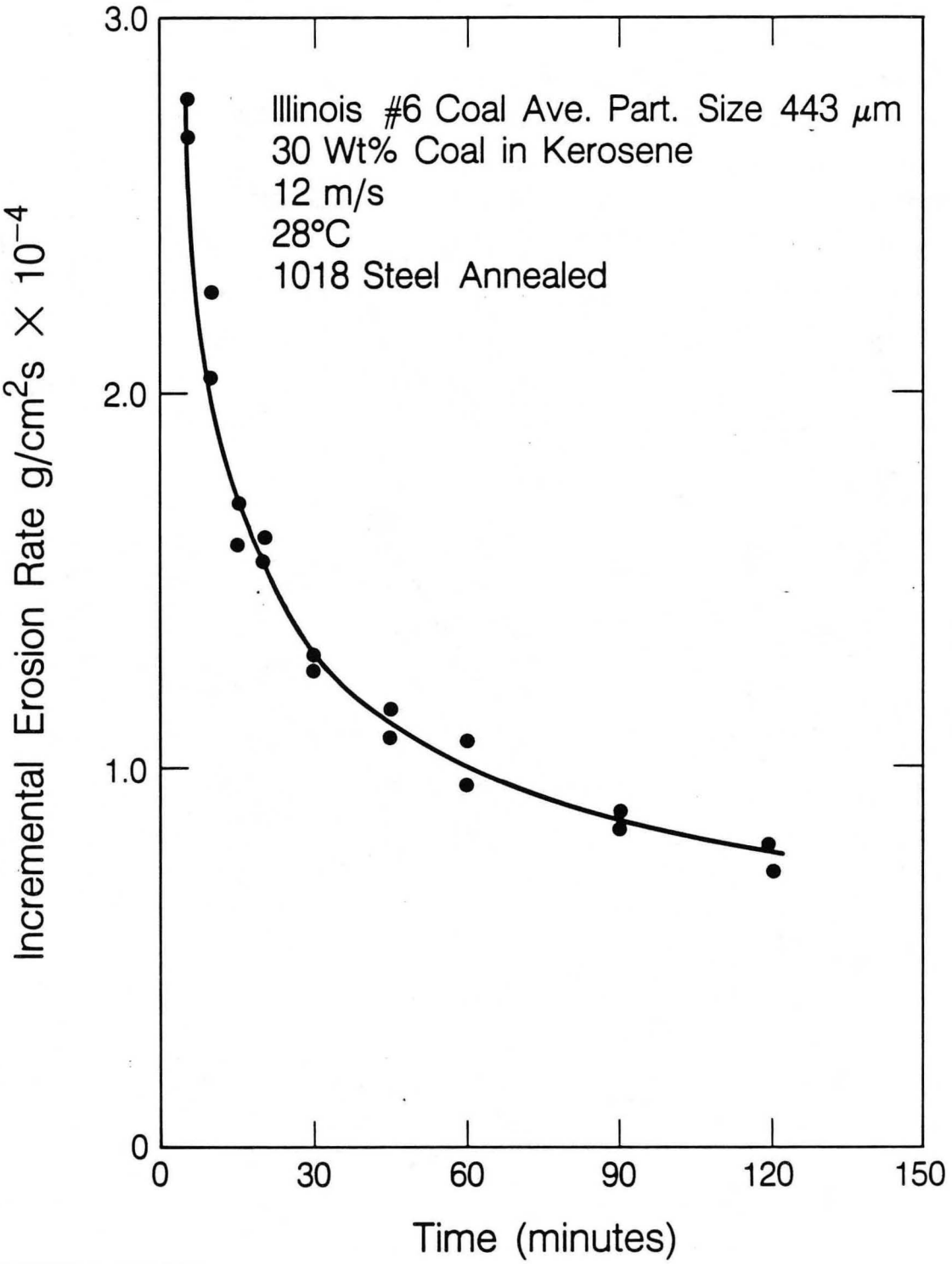

Fig. 4. Incremental erosion rate of 1018 steel by 443μm average diameter Illinois No. 6 coal particles in kerosene.

XBL 846-8971

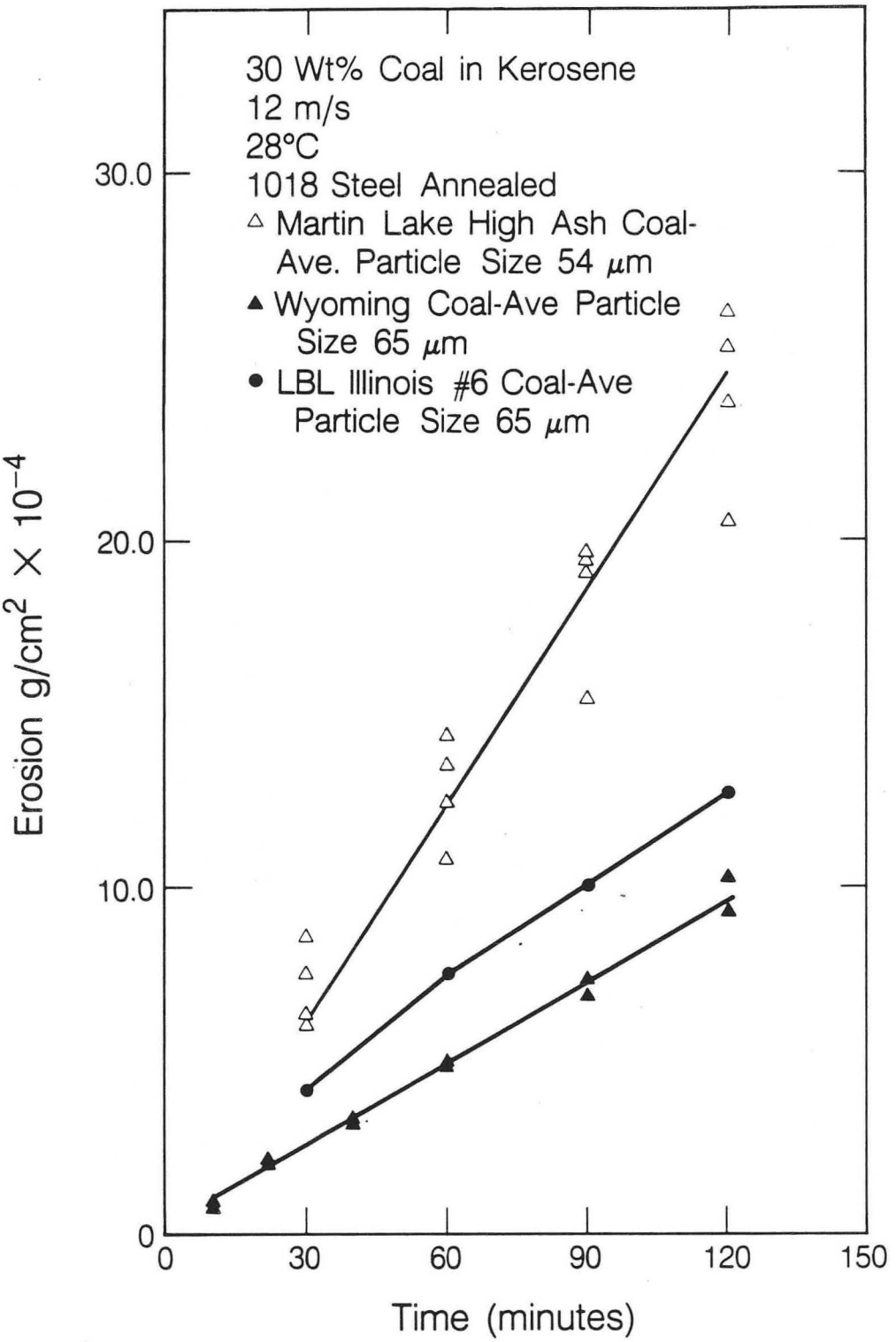

Fig. 5. Cumulative erosion of 1018 steel by 65μm average diameter Illinois No. 6 and Wyoming coal particles in kerosene.

XBL 846-8973

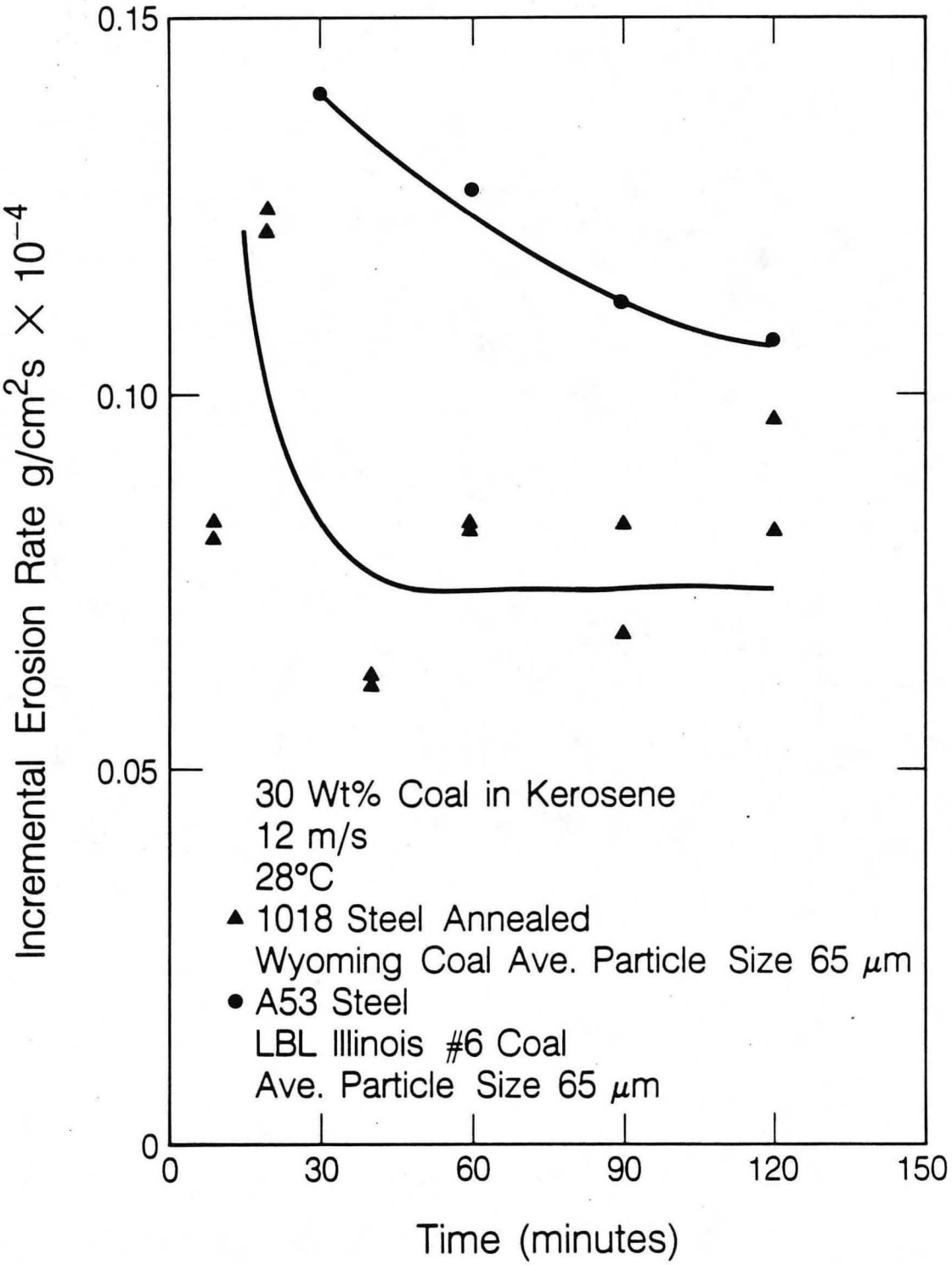

Fig. 6. Incremental erosion rates of 1018 steel by 65μm average diameter Illinois No. 6 and Wyoming coal particles in kerosene.

XBL 846-8972

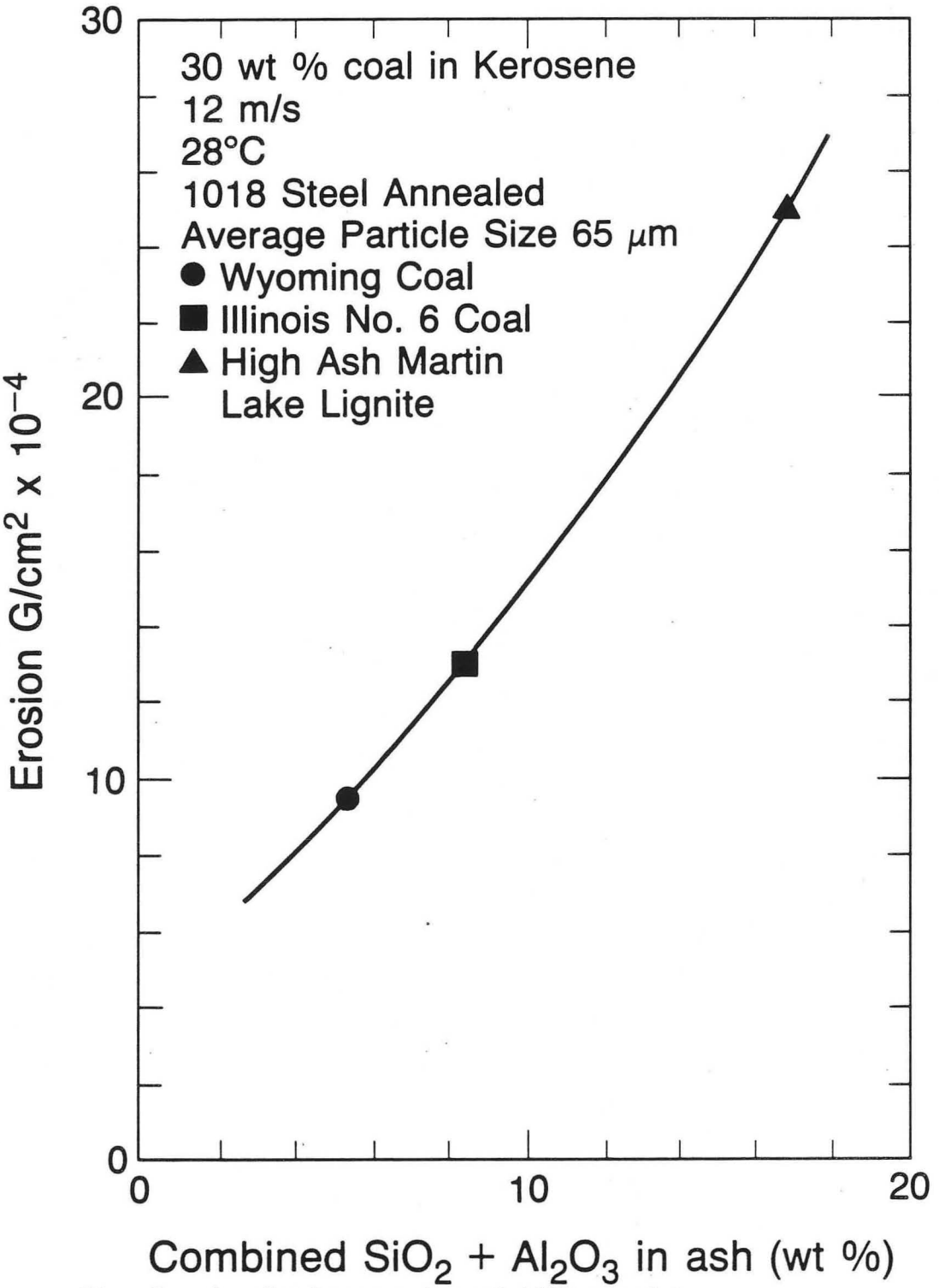

Fig. 7. Cumulative erosion of 1018 steel by Illinois No. 6, Wyoming and High Ash Martin Lake Lignite coals versus the combined SiO_2 + Al_2O_3 content in ash.

XBL 846-10647

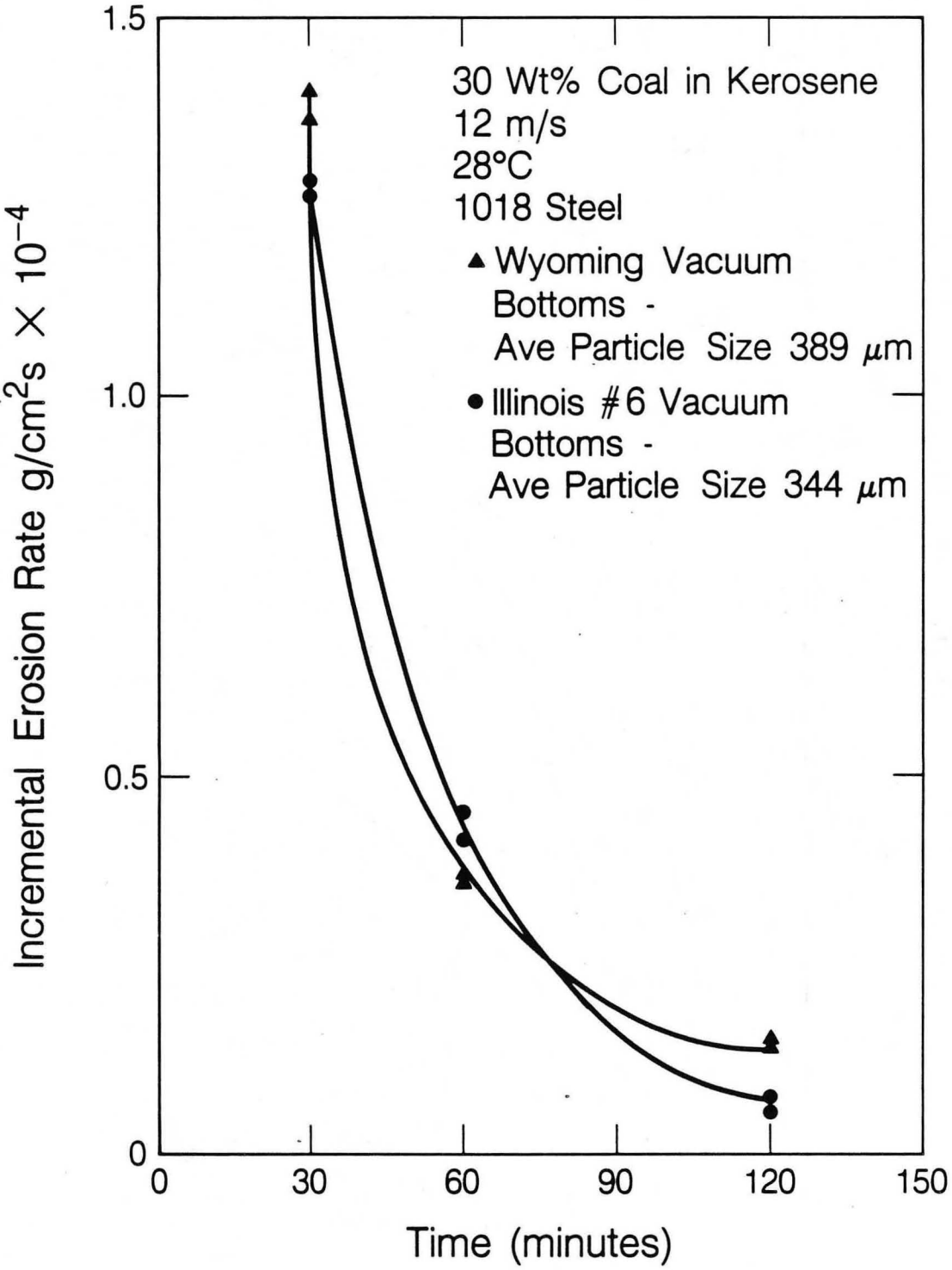

Fig. 8. Incremental erosion rates of 1018 steel by 344μm ave dia Illinois No. 6 and 389μm ave dia Wyoming vacuum bottoms particles in kerosene.

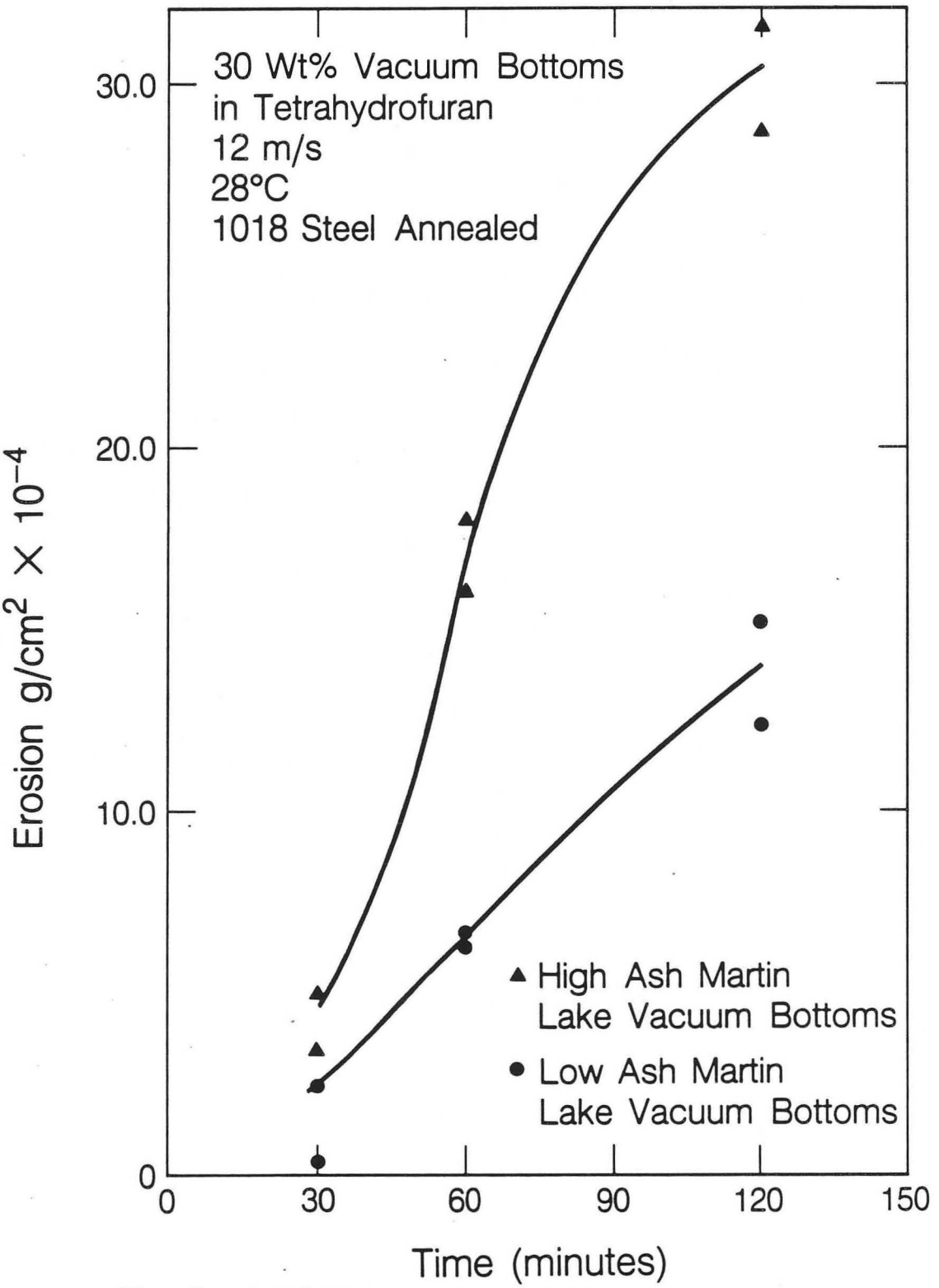

Fig. 9. Cumulative erosion of high and low ash Martin Lake vacuum bottoms in tetrahydrofuran.

XBL 846-8975

DISTRIBUTION LIST

Wate Bakker
EPRI
3214 Hillview Avenue
P.O. Box 10412
Palo Alto, CA 94304

B.R. Banerjee
Ingersoll-Rand Company
P.O. Box 301
Princeton, NJ 08540

K.L. Baumert
Air Products & Chemicals, Inc.
P.O. Box 538
Allentown, PA 18105

S.M. Benford
NASA Lewis Research Center
21000 Brookpark Road
Cleveland, OH 41135

A.E. Biggs
Arco Chemicals
3801 W. Chester Pike
Newtown Square, PA 19073

R. Blickensderfer
Bureau of Mines
P.O. Box 70
Albany, OR 97321

R.A. Bradley, Manager
Fossil Energy Materials Program
Oak Ridge National Laboratory
P.O. Box X
Oak Ridge, TN 37830

Richard Brown
Materials Laboratory
Department of Chemical Engineering
University of Rhode Island
Kingston, RI 02881

DISTRIBUTION LIST cont'd

D.H. Buckley
NASA Lewis Research Center
21000 Brookpark Road
Cleveland, OH 41135

P.T. Carlson, Task Leader
Fossil Energy Materials Program
Oak Ridge National Laboratory
P.O. Box X
Oak Ridge, TN 37830

J. Carpenter
ECUT Program
Oak Ridge National Laboratory
P.O. Box X
Oak Ridge, TN 37830

J.P. Carr
Department of Energy, Office of Fossil Energy
FE-42 Mailstop 3222-GTN
Washington, DC 40525

Hans Conrad
Materials Engineering Department
North Carolina State University
Raleigh, NC 27659

P. Crook
Cabot Corporation
Technology Department
1020 W. Park Avenue
Kokomo, IN 46901

S.J. Dapkunas
Department of Energy, Office of Fossil Energy
Technical Coordination Staff FE-14
Mailstop C-156 GTN
Washington, DC 40525

DOE Technical Information Center
P.O. Box 62
Oak Ridge, TN 37830

W.A. Ellingson
Argonne National Laboratory
9700 South Cass Avenue
Argonne, IL 60439

DISTRIBUTION LIST cont'd

J. Gonzales
GTE
Chemical & Metallurgical Division
Hawes Street
Towanda, PA 18848

Å. Hammarsten
Teknikum
P.O. Box 534, S-751 21
Uppsala
SWEDEN

E. Haycock
Westhollow Research Center
Shell Development Company
P.O. Box 1380
Houston, TX 77001

J.M. Hobday
Department of Energy
Morgantown Energy Technology Center
P.O. Box 880
Morgantown, WV 26505

E.E. Hoffman, Manager
National Materials Program
Department of Energy
Oak Ridge Operations
P.O. Box E
Oak Ridge, TN 37830

J.A.C. Humphrey
Mechanical Engineering Department
University of California
Berkeley, CA 94720

I.M. Hutchings
University of Cambridge
Department of Metallurgy
Pembroke Street
Cambridge
ENGLAND

Sven Jansson
Stal-Laval Turbin AB
Finspong S-61220
SWEDEN

DISTRIBUTION LIST cont'd

R.R. Judkins
Fossil Energy Materials Program
Oak Ridge National Laboratory
P.O. Box X
Oak Ridge, TN 37830

M.K. Keshavan
Union Carbide Corporation
Coating Services Department
1500 Polco Street
Indianapolis, IN 46224

T. Kosel
University of Notre Dame
Dept. of Metallurgical Engineering
& Materials Science
Box E
Notre Dame, IN 46556

L. Lanier
FMC-Central Engineering Laboratory
1185 Coleman Avenue
Santa Clara, CA 95052

N.H. MacMillan
Pennsylvania State University
167 Materials Research Laboratory
University Park, PA 16802

P.K. Mehrotra
Kennemetal Inc.
1011 Old Salem Road
Greensburg, PA 15601

Ken Magee
Bingham-Williamette Co.
2800 N.W. Front Avenue
Portland, OR 97219

T. Mitchell
Case Western Reserve University
Department of Metallurgy
Cleveland, OH 44106

Fred Pettit
Dept. of Metallurgy & Materials Engineering
University of Pittsburgh
Pittsburgh, PA 15261

DISTRIBUTION LIST cont'd

R.A. Rapp
Metallurgical Engineering
116 W. 19th Avenue
The Ohio State University
Columbus, OH 43210

D.A. Rigney
Metallurgical Engineering
116 W. 19th Avenue
The Ohio State University
Columbus,OH 43210

A.W. Ruff
Metallurgy Division
National Bureau of Standards
B-266 Materials
Washington, DC 20234

Alberto Sagüés
IMMR - University of Kentucky
763 Anderson Hall
Lexington, KY 40506

Gordon Sargent
University of Notre Dame
Dept. of Metallurgical Engineering & Materials Science
Box E
Notre Dame, IN 46556

Paul Shewmon
Dept. of Metallurgical Engineering
116 W. 19th Avenue
Columbus, OH 43210

Gerry Sorell
EXXON Research & Engineering Company
P.O. Box 101
Florham Park, NJ 07932

John Stringer
University of California
Lawrence Berkeley Laboratory
Mailstop 62/203
Berkeley, CA 94720

Widen Tabakoff
Dept. of Aerospace Engineering
University of Cincinnati
Cincinnati, OH 45221

DISTRIBUTION LIST cont'd

Edward Vesely
IITRI
10 West 35th Street
Chicato, IL 60616

J.J. Wert
Metallurgy Department
Vanderbilt University
P.O. Box 1621, Sta. B
Nashville, TN 37235

J.C. Williams
Dept. of Metallurgy & Materials Science
Carnegie-Mellon University
Schenley Park
Pittsburgh, PA 15213

S. Wolf
Department of Energy
Basic Energy Sciences Office
Division of Materials Sciences
Washington, DC 20545

Ian Wright
Materials Science Division
Battelle Memorial Institute
505 King Avenue
Columbus, OH 43201

C.S. Yust
Metals and Ceramics Division
Oak Ridge National Laboratory
P.O. Box X
Oak Ridge, TN 37830

TECHNICAL INFORMATION DEPARTMENT
LAWRENCE BERKELEY LABORATORY
UNIVERSITY OF CALIFORNIA
BERKELEY, CALIFORNIA 94720